Protective Performance of Furfuryl Alcohol on 13Cr L80 Steel against Corrosion in Hydrochloric Acid Solution

ARTICLE *in* INDUSTRIAL & ENGINEERING CHEMISTRY RESEARCH · DECEMBER 2013

Impact Factor: 2.59 · DOI: 10.1021/ie4014716

3 AUTHORS, INCLUDING:

Rajeev Puthalath
COLLEGE OF ENGINEERING THALASSERY
2 PUBLICATIONS **6** CITATIONS
SEE PROFILE

A.O. Surendranathan
National Institute of Technology Karnataka
34 PUBLICATIONS **72** CITATIONS
SEE PROFILE

I&EC research
Industrial & Engineering Chemistry Research

Article

pubs.acs.org/IECR

Protective Performance of Furfuryl Alcohol on 13Cr L80 Steel against Corrosion in Hydrochloric Acid Solution

Rajeev Puthalath,*[,†] Attukalathil Orongil Surendranathan,[†] and Chivukula Surya Narayana Murthy[‡]

[†]Department of Metallurgical and Materials Engineering and [‡]Department of Mining Engineering, National Institute of Technology Karnataka, Surathkal, Mangalore 575025, India

ABSTRACT: The search for efficient inhibitors to mitigate the corrosion of oil-well steels requires more experimental investigations of the performance of ecofriendly nontoxic organic inhibitors. With this objective, the inhibitive action of a selected inhibitor, furfuryl alcohol (FAL), on the corrosion resistance of 13Cr L80 steel in 15% HCl solution was investigated using weight-loss, potentiodynamic polarization, and electrochemical impedance spectroscopy (EIS) techniques. The inhibition efficiency of furfuryl alcohol was found to increase almost linearly with concentration and reached about 96% at 90 mM but decreased with temperature. The adsorption of the inhibitor on 13Cr L80 steel in the acidic solution was found to accord with the Langmuir isotherm. Thermodynamic and activation parameters were also evaluated. Scanning electron microscopy (SEM), Fourier transform infrared (FT-IR) spectroscopy, and thermogravimetric analysis (TGA) were carried out to establish the inhibitive properties of FAL. The results from these tests confirmed that FAL is a potential inhibitor for 13Cr L80 steel in HCl acid medium.

1. INTRODUCTION

Oil-well stimulation techniques such as acidization and hydraulic fracturing are important ways of improving the productivity of petroleum reservoirs. Usually, about 15% hydrochloric acid is used for most stimulation jobs. Unfortunately, the corrosive attack of hydrochloric acid on oil-well steels is more severe and aggressive than that of any other acids. To protect oil-well equipment from severe corrosion, inhibitors are commonly used in the petroleum industry during acidization treatments. Organic compounds typically show very good adsorption properties on the metal surface and can therefore be used as effective corrosion inhibitors compared to inorganic compounds.[1] The high performance of such organic corrosion inhibitors is due to the presence of polar functions with S, O, or N atoms; heterocyclic compounds; and π electrons in the molecule. These compounds are adsorbed on the metal surface, blocking the active surface sites and preventing corrosion. Inorganic compounds show good corrosion resistance, but most of them are highly toxic, expensive, and nonbiodegradable.

Corrosion-resistant alloys (CRAs) are generally used to provide long-term resistance to corrosion in the oil and gas industries. Various studies have been conducted using different organic and inorganic compounds on low-alloy steels, but the effectiveness of these inhibitors in protecting high-chromium stainless steel is not satisfactory. The corrosion attack of hydrochloric acid on corrosion-resistant alloys, such as 13Cr and 22Cr stainless steel, is more severe than that on low-alloy steels, especially at temperatures above 65 °C.[1]

Finding a suitable inhibitor for a particular environment depends on many factors and is a difficult process because of the wide variety of corrosive environments.[2] The search for new inhibitors for oil-well stimulation is continuing and needs more evaluations of the inhibitive performances of ecofriendly nontoxic organic inhibitors on oil-well steels. Even though various corrosion inhibition studies have been conducted on N80 steels, studies related to 13Cr L80 steel have been very limited. In a preliminary study, corrosion tests were performed with 13Cr L80, N80, and P110 steels to assess the comparative corrosion resistances of these metals against aggressive attack upon exposure to 15 wt % aqueous hydrochloric acid solutions, and it was found that the corrosion rate was highest for 13Cr L80 steel (Table 1). In the present study, the influence of furfuryl alcohol (FAL) (Figure 1) on the corrosion resistance of 13Cr L80 steel in 15% HCl solution at various concentrations (0−100 mM) was investigated using weight-loss, potentiodynamic polarization, and electrochemical impedance spectroscopy (EIS) techniques. FAL is miscible with water, and upon treatment with acids, it can be made to polymerize into a resin, poly(furfuryl alcohol). FT-IR spectral studies of the surface products formed on 13Cr L80 steel in the inhibited HCl solution were conducted to characterize the compounds responsible for the enhanced corrosion resistance. The thermal stability of the surface products was evaluated by thermogravimetric analysis (TGA). Surface analysis was carried out by scanning electron microscopy (SEM) to supplement the results of corrosion tests.

2. EXPERIMENTAL METHOD

2.1. Material and Medium. 13Cr L80 steel coupons were cut into rectangular pieces with dimensions of 6.0 × 2.0 × 0.3 cm^3 for weight-loss measurements. The chemical composition of the steel coupons is given in Table 1. The samples were polished with different emery papers (400, 600, 800, 1000, 1200, 2000, and 4000), cleaned with acetone, washed with doubly distilled water, and finally dried before all experiments.

Received: May 9, 2013
Revised: November 24, 2013
Accepted: December 11, 2013
Published: December 11, 2013

dx.doi.org/10.1021/ie4014716 | *Ind. Eng. Chem. Res.* 2014, 53, 23−30

Table 1. Compositions of the Metals Supplied by Oil & Natural Gas Commission, Nhava Supply Base, Raigad, Navi Mumbai, India, and Corrosion Rates (CRs) of These Metals in Uninhibited 15% HCl Acid Solution[a]

	alloying elements (wt %)								
metal	Fe	Cr	Mn	Si	C	Ni	P	S	CR (mm year^{-1})
13Cr L80 steel	remainder	13.4	0.428	0.316	0.187	0.134	0.014	0.0022	44.89
L80 steel	remainder	0.190	1.41	0.353	0.263	0.159	0.03	0.001	19.20
N80 steel	remainder	0.21	1.03	0.18	0.318	–	0.017	0.014	22.86
P110 steel	remainder	–	0.71	–	0.16	–	0.002	–	29.87

[a]Analyzed by M/S Servel Engineers Pvt Ltd., Mangalore, India.

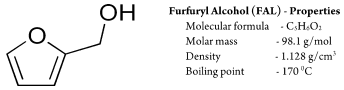

Figure 1. Molecular structure of furfuryl alcohol, containing furan substituted with a hydroxymethyl group.

For electrochemical measurements, the working electrode (WE) was in the form of a disk cut from 13Cr L80 steel and covered by epoxy resin with an exposed area of 1 cm^2. The 15% HCl acid solution was prepared from analytical-reagent-grade of hydrochloric acid and doubly distilled water. Test solutions with volumes of 500 and 200 mL were used for weight-loss and electrochemical measurements, respectively. The test solutions were freshly prepared before each experiment by adding the inhibitor directly to the HCl solution. The standard experimental procedures of corrosion testing[3] were followed for all experiments. Tafel and electrochemical impedance spectroscopy (EIS) experiments were carried out using EC-LAB V10.3 software on a VMP-300 multichannel potentistat at Central Electrochemical Research Institute (CECRI), Karaikudi, India. In all of these experiments, at least three consistent results were considered, and their average values are reported.

2.2. Weight-Loss Method. Cleaned and weighed 13Cr L80 steel samples were completely immersed in a beaker using glass hooks for 6 h. After the experiments, the steel coupons were removed, cleaned with water, rinsed with doubly distilled water, washed with acetone, dried, and weighed.

The corrosion rate (k) and degree of surface coverage (θ) were calculated as

$$k\ (\text{mm·year}^{-1}) = \frac{87.6\Delta W}{DAt} \tag{1}$$

$$\theta = \frac{k_{\text{uninh}} - k_{\text{inh}}}{k_{\text{uninh}}} \tag{2}$$

where ΔW is the weight loss (mg), D is the density of the sample (g cm^{-3}), A is the area of the test coupon (cm^2), t is the exposure time (h), θ is the degree of surface coverage, k_{uninh} is the corrosion rate of the steel coupon in uninhibited acid, and k_{inh} is the corrosion rate of the steel coupon in inhibited acid solution. The experiments from room temperature to 70 °C were carried out at constant temperature (±0.5 °C) using a calibrated thermostat.

2.3. Tafel Polarization and Electrochemical Impedance Spectroscopy (EIS) Studies. Electrochemical experiments were carried out in a glass cell with 200 mL of test solution. A platinum electrode and a saturated calomel electrode (SCE) were used as the counter electrode and reference electrode, respectively. Potentiodynamic polarization curves were plotted at a polarization scan rate of 1 mV s^{-1}. Before all experiments, the potential was stabilized for 30 min. The working electrode, the metal sample, was polarized to −250 mV cathodically and to +250 mV anodically from the rest potential. The electrode potential was plotted against the logarithm of the applied current, and E_{corr} and i_{corr} were determined. The slope of the linear portion of the anodic branch of the polarization curve is the anodic Tafel slope (β_a) and that of the cathodic branch of the porization curve is the cathodic Tafel slope (β_c). The corrosion rate (k) was calculated using the relation

$$k\ (\text{mm·year}^{-1}) = \frac{0.00327E_w i_{\text{corr}}}{D} \tag{3}$$

$$\theta = \frac{i_{\text{corr(uninh)}} - i_{\text{corr(inh)}}}{i_{\text{corr(uninh)}}} \tag{4}$$

$$\eta = \theta \times 100 \tag{5}$$

where E_w is the equivalent weight of the corroding metal, i_{corr} is the current density (μA cm^{-2}), D is the density (g cm^{-3}), θ is the degree of surface coverage, and η is the percentage inhibitor efficiency or protection efficiency. $i_{\text{corr(uninh)}}$ and $i_{\text{corr(inh)}}$ are the current densities for uninhibited and inhibited acid, respectively.

The corrosion behaviors of 13Cr L80 steel in 15% HCl solution in the absence and presence of FAL were also investigated by the EIS method. To understand the interface and surface processes completely, EIS measurements were made at the open-circuit potential (OCP) in a wide frequency range. In the EIS measurements, a small-amplitude ac signal of 10 mV peak-to-peak and a frequency spectrum ranging from 100 kHz to 5 mHz were imposed at the OCP, and impedance data were obtained using Nyquist plots. The inhibition efficiency of the inhibitor was determined from the charge-transfer resistance values using the equation

$$\eta = \frac{R_{\text{ct}} - R_{\text{ct}}^0}{R_{\text{ct}}} \times 100 \tag{6}$$

where R_{ct}^0 and R_{ct} are the charge-transfer resistances for uninhibited and inhibited acid solutions, respectively. The corrosion current density, i_{corr}, was calculated using the charge-transfer resistance (R_{ct}) together with the Stern−Geary equation

$$i_{\text{corr}} = \frac{\beta_a\beta_c}{2.303R_{\text{ct}}A(\beta_a + \beta_c)} \tag{7}$$

where A is the geometric surface area of the electrode and β_a and β_c are the Tafel slopes of the anodic and cathodic processes, respectively.

2.4. Scanning Electron Microscopy (SEM). The surfaces of the metal samples were analyzed by SEM (JEOL model JSM-6380 LA) after the corrosion inhibition experiments with FAL

dx.doi.org/10.1021/ie4014716 | Ind. Eng. Chem. Res. 2014, 53, 23−30

to visualize the inhibitive effect of the inhibitor on the corrosion of 13Cr L80 steel in 15% HCl acid solution.

2.5. FT-IR and Thermal Studies of Corrosion Products. Pure FAL and the products formed on the surface of the metal samples after the corrosion inhibition experiments using FAL were analyzed by Fourier transform infrared (FT-IR) spectroscopy (Bruker Optik Gmbh, Tensor 27, and OPOS version 6.5) and thermogravimetric analysis (TG/DTA 6300, EXSTAR 6000) to characterize the surface products.

3. RESULTS AND DISCUSSION

3.1. Corrosion Measurements. The results of the weight-loss experiments are summarized in Table 2. The results show

Table 2. Corrosion Rates (CRs) of 13Cr L80 Steel Samples and Inhibition Efficiencies (η) of FAL at Different Concentrations

inhibitor concentration (mM)	CR (mm year^{-1})	inhibition efficiency (η, %)
0	44.89	–
10	6.49	85.54
20	4.33	90.35
30	3.21	92.85
40	2.79	93.78
50	2.70	93.98
60	2.68	94.03
70	2.57	94.27
75	2.11	95.30
80	2.01	95.52
85	1.95	95.66
90	1.87	95.83
95	2.02	95.50
100	1.89	95.79

that the 13Cr L80 steel corroded severely in the uninhibited 15% HCl solution, whereas the presence of FAL reduced the dissolution rate considerably. To understand the corrosion inhibition mechanism, the adsorption behavior of FAL molecules on 13Cr L80 steel surface must be known. The values of the degree surface coverage (θ) obtained from weight-loss measurements were used in different isotherm equations, and the best description of the adsorption behavior of FAL was given by the Langmuir isotherm,[4] which can be represented by the equations

$$\frac{\theta}{1-\theta} = K_{ads}C_{inh} \quad (8)$$

$$\frac{C_{inh}}{\theta} = \frac{1}{K_{ads}} + C_{inh} \quad (9)$$

where C_{inh} is the inhibitor concentration of FAL in the HCl solution, K_{ads} is the equilibrium constant of the adsorption process, and θ is the degree of surface coverage. Plots of $\log(C_{inh}/\theta)$ versus $\log(C_{inh})$ gave straight lines with regression coefficients ($R^2 = 0.99979$) almost equal to 1, so the adsorption of FAL on 13Cr L80 steel surface was assumed to follow the Langmuir adsorption isotherm. The fact that the slope (0.95617) of the plot deviated slightly from the value of unity might be due to interactions among the absorbed species. The Langmuir isotherm equation assumes that the absorbed molecules do not interact with each other, but organic molecules with polar atoms or groups can interact by mutual repulsion or attraction.

From the preliminary experiments, it was found that the corrosion rate of 13Cr L80 steel in the inhibitor-free 15% HCl solution was higher than those of N80, L80, and P110 steels (Table 1). As shown in Figure 2, the green color of the acid

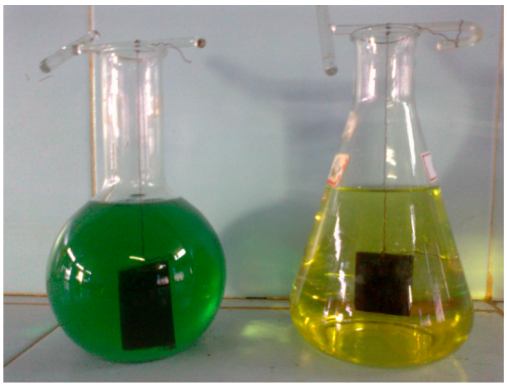

Figure 2. Photographs of (left) 13Cr L80 and (right) L80 steel samples dipped in 15% HCl solution after 6 h of exposure at room temperature (31 °C).

solution containing 13Cr L80 steel is due to the dissolution of the passivating chromium oxide film by the HCl acid. The dissolution rate of 13Cr L 80 steel was found to decrease with time in the inhibitor-free 15% HCl solution and to increase slightly in the presence of FAL (Figure 3). At a concentration

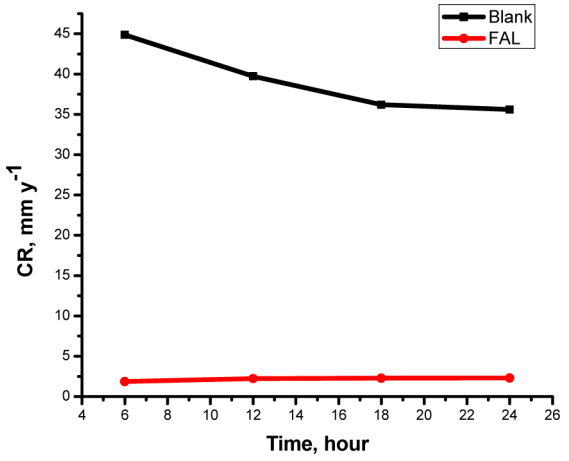

Figure 3. Plot of CR vs t for 13Cr L80 steel in the presence and absence of 90 mM FAL at room temperature (31 °C).

of 90 mM, the inhibition efficiency of FAL was 93.49% after 24 h of exposure in the inhibited acid solution (Table 3 and Figure 4). The inhibition efficiency of FAL decreased with exposure period. This might be due to the partial desorption of the inhibitor molecules from the metal surface.[5] The corrosion rate (CR) increased at elevated temperatures for both the inhibitor-free and inhibited acids. However, the corrosion rate in the presence of FAL was lower than the corrosion rate of the metal in the inhibitor-free acid (Table 4). The inhibition efficiency decreased at elevated temperatures, and 80.56% inhibition was obtained at 70 °C (Table 4 and Figure 5). The lower inhibition at elevated temperature shows the possibility of a higher rate of desorption than adsorption.[6] This might be due to the

dx.doi.org/10.1021/ie4014716 | Ind. Eng. Chem. Res. 2014, 53, 23−30

Table 3. Corrosion Rates (CRs) of 13Cr L80 Steel Samples and Inhibition Efficiencies (η) of 90 mM FAL for Different Exposure Periods at Room Temperature (31 °C)

	CR (mm year^{-1})		
exposure period (h)	blank	FAL	inhibition efficiency (η, %)
6	44.89	1.87	95.83
12	39.75	2.22	94.42
18	36.21	2.29	93.68
24	35.62	2.32	93.49

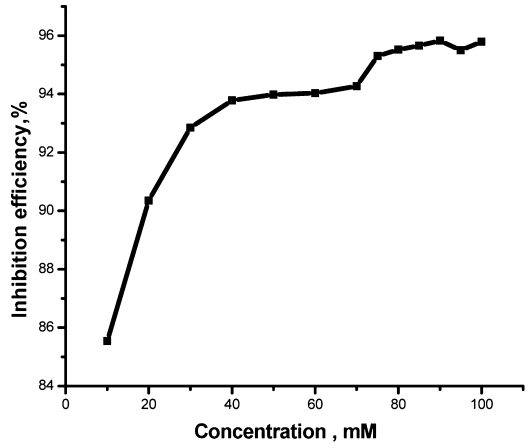

Figure 4. Plot of η vs C for FAL and 13Cr L80 steel at room temperature (31 °C).

Table 4. Corrosion Rates (CRs) of 13Cr L80 Steel and Inhibition Efficiencies (η) of 90 mM FAL at Different Temperatures

	blank	FAL	
temperature (°C)	CR (mm year^{-1})	CR (mm year^{-1})	inhibition efficiency (η, %)
31	44.89	1.87	95.83
40	68.60	6.12	91.08
50	98.48	12.76	87.04
60	288.20	54.50	81.09
70	875.59	170.23	80.56

increased solution agitation resulting from higher rates of hydrogen gas evolution, which might reduce the strength of the adsorption process at elevated temperatures, suggesting the physical adsorption of FAL on the 13Cr L80 steel surface.[7]

Figure 6 presents a Tafel plot for the corrosion of 13Cr L80 steel inhibited by different concentrations of FAL at room temperature (31 °C). The maximum inhibition efficiency (98.26%) was achieved at a 90 mM concentration of FAL. Potentiodynamic polarization parameters such as corrosion potential (E_{corr}), corrosion current density (i_{corr}), anodic slope (β_a), cathodic slope (β_c), and corrosion rate (CR) were obtained from the Tafel plot and are reported in Table 5. The results indicate that increasing concentrations of FAL shifted the polarization curves to the high-current-density region, indicating an increase in the corrosion rate. The corrosion potential in the presence of FAL shifted slightly toward the positive side. This observation indicates that the inhibitor is acting on anodic areas. The shift of the Tafel slopes indicates that the mixed type of inhibition is offered by FAL. A Nyquist plot for the corrosion of 13Cr L80 steel in 15% HCl solution at different concentrations of FAL at room temperature (31 °C) is shown in Figure 7. The semicircles in the impedance diagram indicate that the corrosion process is mainly controlled by the charge-transfer process. The main impedance parameters obtained are listed in Table 6. The equivalent circuit used for the EIS data, consisting of five elements, is shown in Figure 8. As can be seen from the table, with increasing concentration of FAL, the measured values of charge-transfer resistance (R_{ct})

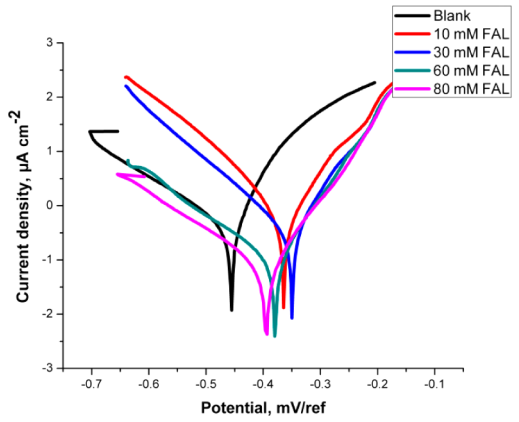

Figure 6. Tafel plot for 13Cr L80 steel in 15% HCl solution containing FAL at different concentrations.

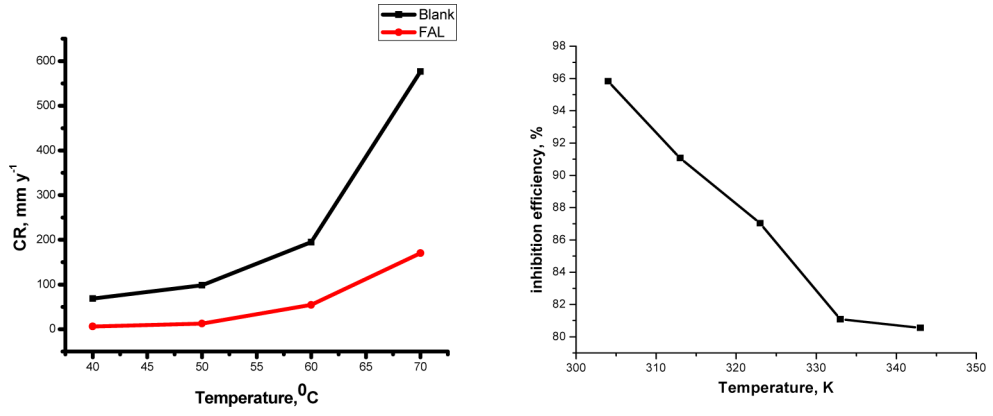

Figure 5. Plots of CR vs T and η vs T for 13Cr L80 steel with 90 mM FAL in the inhibited and uninhibited acid after 6 h of exposure in 15% HCl solution.

dx.doi.org/10.1021/ie4014716 | Ind. Eng. Chem. Res. 2014, 53, 23−30

Table 5. Corrosion Rates and Inhibition Efficiencies Obtained from Potentiodynamic Polarization Tests for 13Cr L80 Steel in 15% HCl Containing Various Concentrations of FAL at Room Temperature (31 °C)

					Tafel slopes	
C (mM)	CR (mm year^{-1})	η (%)	E_0 (mV)	i_0 (μA cm^{-2})	β_a (mV dec^{-1})	β_c (mV dec^{-1})
0	45.85	–	−428.645	4285.021	131.6	−123.5
10	7.422	83.81	−362.78	593.678	79.3	−102.0
30	3.53	92.3	−349.9	330.108	78.3	−122.5
60	0.9723	97.88	−378.915	90.87	65.6	−137.6
80	0.799	98.26	−394.559	74.677	76.7	−150.7

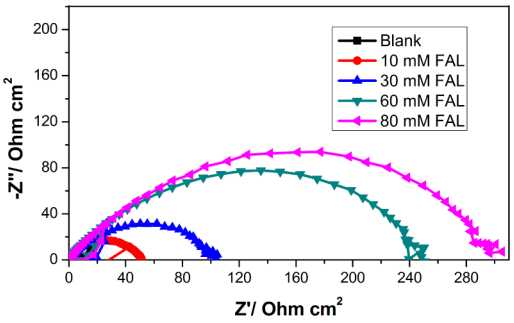

Figure 7. Nyquist plot for 13Cr L80 steel in 15% HCl solution containing FAL at different concentrations.

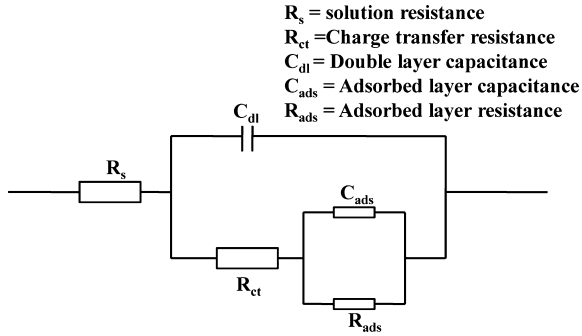

Figure 8. Equivalent circuit used in modeling EIS data for FAL.

increased, and the values of the double-layer capacitance (C_{dl}) decreased. The increases in the values of R_{ct} and inhibition efficiency are due to the formation of a protective surface film on the metal surface caused by the gradual replacement of water molecules by adsorbed inhibitor molecules. As a result, the thickness of the electronic double layer increased, and the electrical capacitance decreased.[8] The decrease in C_{dl} occurred as a result of the decrease in the local dielectric constant, which suggests that FAL molecules function by adsorption.[9]

The inhibition efficiencies obtained from different testing methods used in this study are comparable and in fair agreement.

3.2. Scanning Electron Microscopy. Figure 9a shows an SEM image of a 13Cr L80 steel specimen exposed to 15% HCl solution for 6 h at room temperature. The image shows the severity of the corrosion attack on the metal sample. In contrast, as shown in Figure 9b, the metal surface is comparatively smooth and free from corrosion attack in the presence of FAL. This result supplements the results of other corrosion tests and confirms that FAL inhibits the corrosion of 13Cr L80 steel through adsorption of the inhibitor on the metal surface.

3.3. FT-IR Analysis and TGA Results. The FT-IR spectrum (Figure 10) of the surface product obtained from 13Cr L80 steel sample exposed to 15% HCl for 6 h in the presence of FAL showed a broad band at 3394 cm^{-1}, and a broad band at 3367 cm^{-1} was observed for pure FAL, which can be assigned to the presence of O−H stretching in both cases. The peak at 1619 cm^{-1} for the metal surface product might be due to the stretching of furan rings, whereas the infrared spectrum for pure FAL showed a peak at 1609 cm^{-1}. The peaks observed at 1619 and 1416 cm^{-1} (1609 and 1422 cm^{-1} for FAL) can be assigned to the presence of aliphatic segments. The peaks observed at 3394, 1619, 1416, 1212, 1016, 966, 786, and 595 cm^{-1} for the metal surface product (at 3367, 1609, 1422, 1217, 1010, 916, 816, and 599 cm^{-1} for pure FAL) might reveal the presence of furan rings in the polymeric compound.[10−21]

The thermograms obtained for the surface products formed on the 13Cr L80 steel samples after the corrosion tests are shown in Figure 11. The thermograms show that the initial weight loss started very slowly, which might be due to the volatilization of absorbed HCl acid and moisture. The curves fall at 90−130 °C as a result of the degradation of the surface products at these temperatures. The results show that pure FAL and the surface products are thermally stable up to 130 °C.

3.4. Kinetic/Thermodynamic Studies. Thermodynamic and activation parameters were used to ascertain the inhibitive mechanism of the inhibitor. As explained in section 3.1 the experimental results were best fit with the Langmuir adsorption isotherm. The inhibitor efficiencies obtained in the presence of 90 mM FAL at different temperatures (Table 4) showed that increasing the temperature increased the corrosion rate and decreased the inhibitor efficiency. These results indicate that

Table 6. Electrochemical Corrosion and Impedance Parameters Obtained from EIS Studies for 13Cr L80 Steel in 15% HCl Solution Containing Different Concentrations of FAL at Room Temperature (31 °C)

inhibitor concentration (mM)	i_{corr} (μA cm^{-2})	CR (mm year^{-1})	R_{ct} (Ω cm^2)	C_{dl} (μF cm^{-2})	η (%)
0	4046.810	43.270	8.809	360.80	–
10	483.508	5.170	50.910	123.10	82.71
30	251.430	2.687	102.600	50.53	91.41
60	91.740	0.982	242.500	52.09	96.37
80	81.360	0.870	300.400	66.81	97.07

dx.doi.org/10.1021/ie4014716 | Ind. Eng. Chem. Res. 2014, 53, 23−30

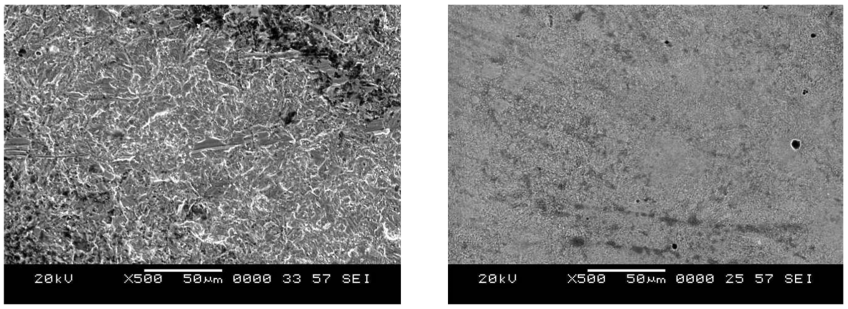

(a) (b)

Figure 9. SEM images of 13Cr L80 steel surfaces after 6 h of exposure in 15% HCl solution at room temperature (a) in plain solution and (b) in the presence of 90 mM FAL.

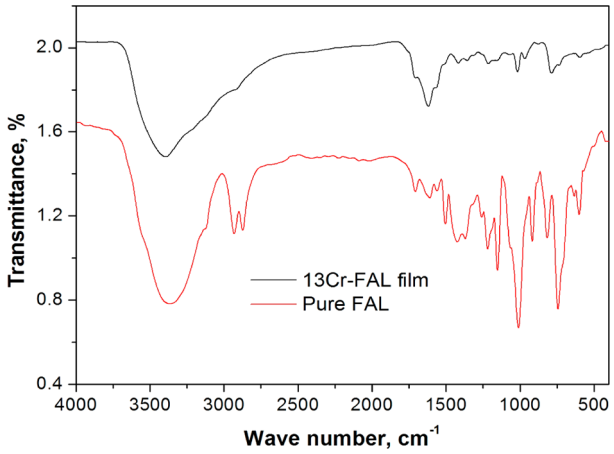

Figure 10. FT-IR spectra of the corrosion product formed on 13Cr L80 steel in 15% HCl containing 90 mM FAL and of pure FAL alone.

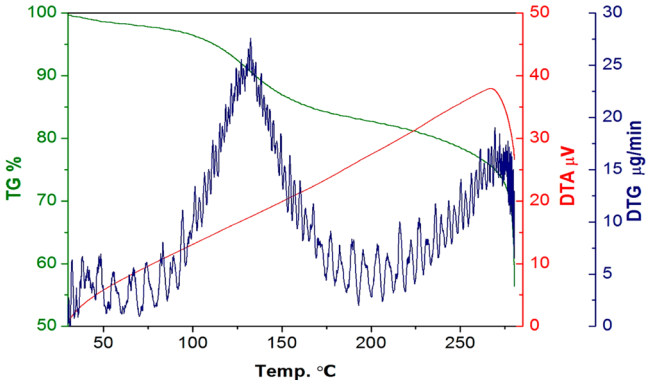

Figure 11. TGA curve of the metal surface product obtained after immersion of 13Cr L80 steel in 15% HCl solution containing 90 mM FAL.

FAL was adsorbed on the 13Cr L80 steel surface physically and that the rate of the adsorption process decreased at elevated temperatures. Activation parameters such as the energy (E_a), enthalpy (ΔH^*), and entropy (ΔS^*) of activation for the dissolution of 13Cr L80 steel in the inhibited HCl solution were obtained from the Arrhenius equation

$$k = Ae^{-E_a/RT} \tag{10}$$

and the transition-state equation[22−24]

$$k = \frac{RT}{Nh} e^{\Delta S^*/R} e^{\Delta H^*/RT} \tag{11}$$

where k is the corrosion rate, A is the Arrhenius pre-exponential factor, E_a is the apparent effective activation energy, R is the universal gas constant, T is the absolute temperature, h is Planck's constant, and N is Avogadro's number. A plot of the logarithm of the corrosion rate (k) obtained by the weight-loss method versus $1/T$ gave a straight line, and the value of E_a was calculated from the slope of the obtained straight line for both the cases of inhibitor-free acid and inhibited acid.

The value of the free energy of adsorption (ΔG_{ads}) can be obtained from the relationship

$$K_{eq} = \frac{1}{55.5} \exp\left(\frac{-\Delta G_{ads}}{RT}\right) \tag{12}$$

Table 7 shows that E_a increased when FAL was added, which indicates the concurrent increase in the energy barrier of the activated complex for the corrosion reaction. The fact that the activation energy (E_a) of the corrosion process is over 20 kJ mol^{-1} indicates that the whole process is under the surface reaction control.[25−27] The negative value of ΔG_{ads} suggests (Table 7) that the adsorption of inhibitor molecules onto the steel surface is a spontaneous phenomenon and that the adsorbed layer on the 13Cr L80 steel surface is stable.[9,27,28] Values of ΔG_{ads} around −20 kJ mol^{-1} or lower are associated with electrostatic interactions between charged molecules and a charged metal, which indicates physisorption, whereas those around −40 kJ mol^{-1} or higher are associated with chemisorption, in which the sharing or transfer of electrons from organic molecules to the metal surface occurs. Here, the calculated value of ΔG_{ads} is −37.86 kJ mol^{-1}, indicating that the adsorption mechanism of FAL on 13Cr L80 steel might be a combination of both electrostatic adsorption and chemisorption (comprehensive adsorption).[8] However, physisorption is the major contributor, whereas the contribution by chemisorption to the adsorption mechanism is less, given that an increase in temperature decreased the value of η. The values of the enthalpy (ΔH^*) and entropy (ΔS^*) of activation of the

Table 7. Thermodynamic and Activation Parameters of FAL in 15% HCl Solution for 13Cr L80 Steel

inhibitor	E_a (kJ mol^{-1})	ΔG_{ads} (kJ mol^{-1})	ΔS^* (J mol^{-1} K^{-1})	ΔH^* (kJ mol^{-1})
blank	64.608	–	−11.907	61.937
FAL	98.392	−37.86	74.648	95.723

dx.doi.org/10.1021/ie4014716 | Ind. Eng. Chem. Res. 2014, 53, 23−30

corrosion process were obtained from the alternative form of Arrhenius equation (the transition-state equation)[9]

$$k = \frac{RT}{Nh} \exp(\Delta S^*/R) \exp(-\Delta H^*/RT) \quad (13)$$

where h is Planck's constant, N is Avogadro's number, ΔS^* is the entropy of activation, and ΔH^* is the enthalpy of activation. ΔS^* and ΔH^* were calculated from the intercept and slope, respectively, of a plot of $\log(k/T)$ versus $1/T$ (Figure 12).

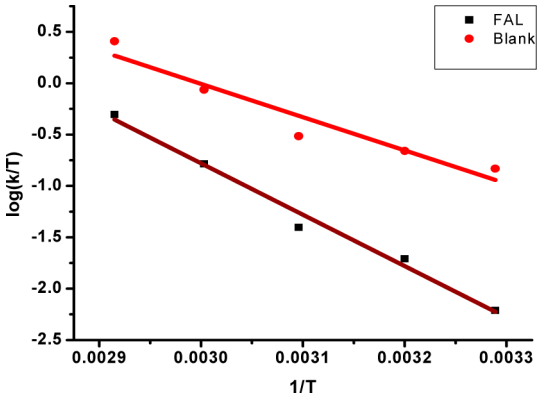

Figure 12. $\log(k/T)$ vs $(1/T)$ plot for 13Cr L80 steel corrosion in 15% HCl solution in the absence and presence of the optimum concentration of FAL.

The positive value of the enthalpy of activation (ΔH^*) indicates that the corrosion process is an endothermic phenomenon and that the dissolution of steel is difficult.[22] The values of ΔH^* and E_a were found to be nearly the same and higher in the presence of the inhibitor. This indicates that the energy barrier of the corrosion reaction increased in the presence of the inhibitor. The positive value of ΔS^* in the presence of FAL is an indication of an increase in solvent entropy. It also indicates an increase in disorder due to the presence of more water molecules, which can be desorbed from the metal surface by one inhibitor molecule.[9] In the presence of the inhibitor, the value of ΔS^* increases and is generally interpreted as an increase in disorder as the reactants are converted into activated complexes.[29]

4. CONCLUSIONS

- The corrosion rate of 13Cr L80 steel in 15% HCl solution is substantial, and FAL behaves as an efficient inhibitor.
- The protective efficiency of FAL increased with increasing concentration and reached 95.83% at a 90 mM concentration at room temperature, but it decreased with increasing exposure time and temperature.
- The adsorption of FAL on the metal surface obeyed the Langmuir adsorption isotherm.
- FAL preferentially acted on anodic areas. The shift of the Tafel slopes indicated that the mixed type of inhibition was offered by FAL.
- An FT-IR spectral study showed the presence of inhibitor molecules on the metal surface after exposure in the inhibited acid solution, which indicates the formation of a surface film on the surface.
- TGA revealed that the surface products obtained from the metal surface are thermally stable up to 130 0C.

AUTHOR INFORMATION

Corresponding Author

*Tel.: 08547519386. E-mail: puthalathkannur@yahoo.co.in.

Notes

The authors declare no competing financial interest.

ACKNOWLEDGMENTS

The authors express deep gratitude to Dr. L. John Berchmans, Scientist, CECRI, Karaikudy, India, for help and support by granting permission to use the laboratory facilities of CECRI.

REFERENCES

(1) Menezes, M. A. M.; Valle, M. L. M.; Dweck, J.; Queiroz Neto, J. C. Temperature dependence of corrosion inhibition of steels used in oil well stimulation using acetylene compound and halide ions salt mixture. *Braz. J. Pet. Gas* **2007**, *1*, 8−15.

(2) Khamis, E. The effect of temperature on the acidic dissolution of steel in the presence of inhibitors. *Corrosion* **1990**, *46*, 476−484.

(3) Ailor, W. H. *Handbook on Corrosion Testing and Evaluation*; John Wiley & Sons: New York, 1971.

(4) Paul, S.; Kar, B. Mitigation of mild steel corrosion in acid by green inhibitors yeast, pepper, garlic and coffee. *ISRN Corrosion* **2012**, *2012*, 641386−8.

(5) Vishwanatham, S.; Haldar, N. Furfuryl alcohol as corrosion inhibitor for N80 steel in hydrochloric acid. *Corros. Sci.* **2008**, *50*, 2999−3004.

(6) Okafor, P. C.; Liu, C. B.; Liu, X.; Zheng, Y. G.; Wang, F.; Lin, C. Y. Corrosion inhibition and adsorption behavior of imidazoline salt on N80 carbon steel in CO_2 saturated solution and its synergism with thiourea. *J. Solid State Electrochem.* **2009**, *14*, 1367−1376.

(7) Oguzie, E. E. Corrosion inhibition of aluminum in acidic and alkaline media by *Sansevieria trisfasciata* extract. *Corros. Sci.* **2007**, *49*, 1527−1539.

(8) El-Taib Heakal, F.; Fouda, A. S.; Radwan, M. S. Some new thiadiazole derivatives as corrosion inhibitors for 1018 carbon steel dissolution in sodium chloride solution. *Int. J. Electrochem. Sci.* **2011**, *6*, 3140−3163.

(9) Shukla, S. K.; Ebenso, E. E. Corrosion inhibition, adsorption behavior and thermodynamic properties of streptomycin on mild steel in hydrochloric acid medium. *Int. J. Electrochem. Sci.* **2011**, *6*, 3277−3291.

(10) Stoner-Ma, D.; Jaye, A. A.; Matousek, P.; Towrie, M.; Meech, S. R.; Tonge, P. J. Observation of excited state proton transfer in green fluorescent protein using ultrafast vibrational spectroscopy. *J. Am. Chem. Soc.* **2005**, *127*, 2864−2865.

(11) Costa, L. B.; Del Boghi, M.; Deluchi, G.; Fumagalli, M.; Drachev, A. and Gilman, A. IR detailed investigation on the polymer structures obtained from 3-methoxythiophene by plasma polymerization and poly-3,3[1]-dipenlhoxy-2,2[1]-bithiophene produced by the classical chemical synthesis. Presented at *ISTAPC-2008*, Ivanovo, Russia, Sep 3−8, 2008.

(12) Beauchamp, P. Spectroscopy Data Tables, Infrared Tables (short summary of common absorption frequencies); California State Polytechnic University, Pomona, CA. www.csupomona.edu/~psbeauchamp/pdf/424_spectra_tables.pdf.

(13) Librando, V.; Minniti, Z.; Lorusso, S. Ancient and modern paper characterization by FT-IR and micro-Raman spectroscopy. *Conserv. Sci. Cultural Heritage* **2011**, *11*, 249−263.

(14) Huang, R.; Gao, H.; Tang, Y.; Liu, Q. Curing mechanism of furan resin modified with different agents and their thermal strength. *China Foundry* **2011**, *8*, 161−165.

(15) Tian, Q.; Yuan, Y. C.; Rong, M. Z.; Zhang, M. Q. A thermally remendable epoxy resin. *J. Mater. Chem.* **2009**, *19*, 1289−1296.

(16) Gopakumar, B.; Narayanaswamy. Fourier Transform-Infrared (FT-IR) spectra analysis of root rot disease in sesame. *Rom. J. Biophys.* **2008**, *18*, 217−223.

(17) Fujil, S.; Osawa, Y.; Suginuira, H. Infrared spectra of Japanese coal. The absorption bands at 3030, 2920 and 1600 cm^{-1}. *Fuel* **1970**, *49*, 68−74.
(18) Bellamy, L. J. *The Infrared Spectra of Complex Molecules*; Chapman & Hall: London, 1975.
(19) Hlaing Oo, W. M. Infrared spectroscopy of zinc oxide and magnesium nanostructures. Ph.D. Thesis, Washington State University, Pullman, WA, 2007.
(20) Maruthamuthu, S.; Mohanan, S.; Rajasekar, A.; Muthukumar, N.; Ponmarippan, S.; Subramanian, P.; Palaniswamy, N. Role of corrosion inhibitor on bacterial corrosion in petroleum product pipelines. *Indian J. Chem. Technol.* **2005**, *12*, 567−575.
(21) Smith, B. C. *Fundamentals of Fourier Transform Infrared Spectroscopy*; CRC Press: Boca Raton, FL, 2011; pp 90−170.
(22) Ebenso, E. E. Inhibitive properties, thermodynamic characterization and quantum chemical studies of secnidazole on mild steel corrosion in acidic medium. *Int. J. Electrochem. Sci.* **2010**, *5*, 2012−2035.
(23) Khedr, M. G. A.; Lashien, A. M. S. The role of metal cations in the corrosion and corrosion inhibition of aluminium in aqueous solutions. *Corros. Sci.* **1992**, *33*, 137−151.
(24) Solomon, M. M.; Umoren, S. A.; Udousoro, I. I.; Udoh, A. Inhibitive and adsorption behaviors of carboxymethyl cellulose on mild steel corrosion in sulphuric acid solution. *Corros. Sci.* **2010**, *52*, 1317−1325.
(25) Maatya, A. K.; Al-Rawarshdeh, N. A. F. Inhibition of acidic corrosion of pure aluminium by some organic compounds. *Corros. Sci.* **2004**, *46*, 1129−1140.
(26) Abboud, Y.; Abourriche, A.; Sattaj, T.; Berrada, M.; Charrouf, M.; Bennamara, A.; Hennache, H. A novel azo dye, 8-quinolinol-5-azoantipyrite as corrosion inhibitor for mild steel in acidic media. *Desalination* **2009**, *237*, 175−189.
(27) El-Taib Heakal, F.; Fouda, A. S.; Radwan, M. S. Inhibitive effect of some thiadiazole derivatives on C-steel corrosion in neutral sodium chloride solution. *Mater. Chem. Phys.* **2011**, *125*, 26−36.
(28) Fouda, A. S.; Elewady, G. Y.; El-Haddad, M. N. Corrosion inhibition of carbon steel in acidic solution using some azodyes. *Can. J. Sci. Ind. Res.* **2011**, *2*, 1−9.
(29) Zarrok, H.; Oudda, H.; Zarrouk, A.; Salghi, R.; Hammouti, B.; Bouachrine, M. Weight loss measurement and theoretical study of new pyridazine compound as corrosion inhibitor for C38 steel in hydrochloric acid solution. *Pharma Chem.* **2011**, *3*, 576−590.